Impulse-Momentum Analysis of Multibody Vehicle-Pedestrian Collision Simulations

Raymond M. Brach, PhD, PE,
Professor Emeritus, University of Notre Dame, USA

Abstract

For purposes of vehicle-pedestrian crash simulation, vehicle speed, vehicle-pedestrian interaction and pedestrian motion are currently related using one of three model types. Such models relate vehicle speed to: I) throw distance alone (through experimental data and/or mechanics), II) to throw distance and vehicle and roadway parameters such as launch angle, pedestrian-ground drag coefficient and travel distance, vehicle frontal geometry, etc. and III) the use of pedestrian multibody models and vehicle finite element structural parameters. This paper presents a comparison of Type II model results to a set of multibody, Type III model results. The Type II model uses point-mass impact mechanics to model the vehicle-pedestrian contact phase through the use of impact parameters, namely the coefficient of restitution and impulse ratio. Frontal vehicle geometry such as the vehicle's hood/bonnet slope and leading edge height is taken into account. Through the use of least-square methods, the Type II model is used to determine the impact parameters corresponding to the Type III MADYMO model simulations published in the 2012 IRCOBI proceedings by Hamacher, et al. These parameters provide an indication of how the MADYMO simulations satisfy Newton's laws in the form of impulse and momentum and provide a kinetic energy accountability.

It is shown that the Type II model is capable of producing kinematic results identical or very close to MADYMO simulations including the pedestrian launch angle, launch speed and throw distance. The main finding from comparisons of simulations with impact equation solutions, is that these MADYMO simulations tend to display the counterintuitive trend that as vehicle speeds increase, the percentage of kinetic energy lost during the vehicle-pedestrian contact phase decreases. Such trends are opposite to what is found in the literature for mechanical impacts.

Zusammenfassung

from 100 to 300 words **(in German)** – shortly explain the problem, methods of solution and basic results).

Introduction

In current literature, vehicle-pedestrian throw-distance models typically are categorized according to whether they are based directly on test data (regression equations), whether they are derived using principles of mechanics or if they use multibody pedestrian mechanics (and/or finite element methods). A thorough review of such-categorized models is not given here because many already exist [1, 2, 3, 4]. An alternative model categorization is proposed here, based on level of model complexity. The simplest (Type I) are those models that relate vehicle speed to pedestrian throw distance using a single equation (i.e. formula). Such models can be based on mechanics, statistical analysis of test data, or can be based on both, sometimes referred to as hybrids. A fairly complete collection of such models exists [5]. Type II models are defined as those that include parameters representing the contact of the vehicle and pedestrian, the distance of travel of the pedestrian through the air (ballistic trajectory), the movement of the pedestrian along the ground to rest and the postimpact motion of the vehicle [4, 6-9]. The final category, Type III, consists of multibody models [4]. Two such models typically referenced in the literature are PC-Crash [10] and MADYMO [11]. A newer type of Type II model is now beginning to appear in the literature [12,13] based on fuzzy mathematics.

It should also be pointed out that different categories, or classifications, of vehicle-pedestrian ***crash configurations*** are covered in the literature [14, 15]. The most common ones are wrap, forward projection, fender vault, roof vault and somersault. Most Type I and Type II models are limited to application to wrap and forward projection collisions. This is true for the Type II model developed here. However such a restriction is due not so much to the model characteristics but rather to a lack of validation test data for the other classes of crashes.

Work similar to what is presented here has been published in the past. Bhalla et al., [1] present comparisons of MADYMO simulations to results of two Type I models. For a range of impact conditions they find high uncertainty from the Type I formula results because the formulas omit variables such as relative pedestrian-vehicle geometry, pedestrian preimpact orientation, and pedestrian-roadway frictional drag characteristics. Some of those deficiencies are corrected through the use of the Type II model in the following.

The work by Hamacher, et al. [16] includes a description of a comprehensive set of results of MADYMO simulations of combinations of frontal vehicle-pedestrian crashes involving six types of vehicles (compact, sedan, van, sports car, SUV, and OneBox) and four pedestrian models (6 year-old child, 5%ile female, 50%ile male and 95%ile male). Emphasis is on the postimpact pedestrian kinematics. Simulation results include: flight altitude, throw distance, launch speed and launch angle. The approach taken in this paper is to match some of the MADYMO results (Type III) to results of the point-mass Type II impact model using the method of minimization of least-square differences to find the two vehicle-pedestrian impact parameters, namely the coefficient of restitution and impulse ratio [17, 18, 22]. Values of the coefficient of restitution and the impulse ratio (effective coefficient of friction) for each MADYMO simulation are calculated to provide an indication of how each simulation satisfies the equations of impact mechanics.

Two issues are discussed here concerning model validation. First, because of their simplicity, Type I and II models are often used to reconstruct vehicle-pedestrian accidents. A very important concept must be recognized concerning uncertainty for use in specific accident reconstruction. Models generally are validated by comparison of their output with data collected from experimental tests [4]. (Other types of validation are used [12]). Once a model is validated, the variations in the experimental data used for validation become irrelevant when the model is applied to the reconstruction of a specific accident. The irrelevancy makes sense when the source of test variations is recognized as being from a variety of test dummies, a variety of vehicles, a variety of roadway conditions, a variety of data collection techniques, etc. On the other hand, reconstruction uncertainty is a matter of how closely the model's parameters match the specific accident being reconstructed. The second issue to discuss is that this paper compares the results of two models. As such this comparison does not constitute a validation of either model. Validations of various facets of the MADYMO model such as biofidelity and head motion have been published [4, 19, 20, 21].

Vehicle-Pedestrian Throw Model

The Han-Brach pedestrian throw model was originally introduced in 2001 [8]. To use the model, the pedestrian's velocity and launch angle had to be specified. Since then, the model has been enhanced using point-mass impact mechanics and the vehicle's hood/bonnet slope and height as input to determine the pedestrian launch velocity and direction. This is a Type II model that takes into account the aerial trajectory following launch, the effects of the impact of the pedestrian with the ground (roadway) and the motion of the pedestrian along the ground to rest. Figure 1 is a diagram which shows coordinates and variables corresponding to the Han-Brach throw model.

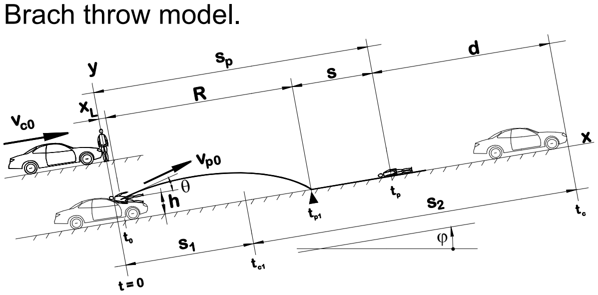

Figure 1. Diagram of a vehicle-pedestrian collision showing coordinates and variables

The conceptual events on which the vehicle-pedestrian impact mechanics are based are illustrated in Figure 2, showing a wrap collision. From initial contact to when the pedestrian moves in the direction of the vehicle, a momentum change takes place where the vehicle loses speed and the pedestrian is accelerated to a speed nearly equal to the vehicle. Shortly after initial contact with the front of the vehicle (bumper, grille), the pedestrian's body wraps up onto the hood/bonnet with an additional momentum transfer [17, 18, 22].

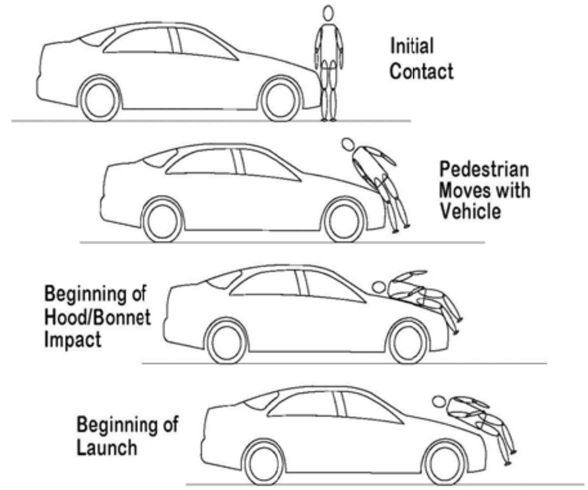

Figure 2. Sequence of events of a wrap vehicle-pedestrian collision.

This interaction is followed by the launch as the vehicle is decelerated. It is assumed that after the launch no further contact takes place between the pedestrian and vehicle. The final conditions of the impact are the initial conditions of the launch. If the center of gravity of the pedestrian (modeled as a point mass) lies below the height, *b*, of the hood/bonnet leading edge (see Figure 3), the launch angle can be zero and pedestrian is launched horizontally (typically referred to as a frontal projection).

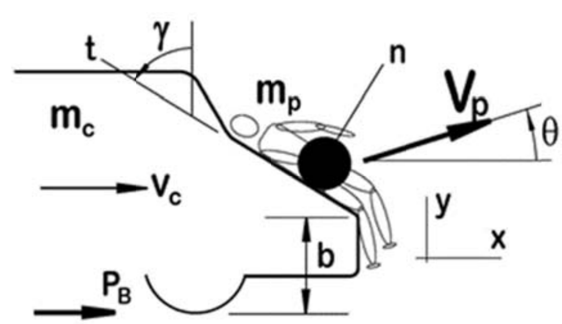

Figure 3. Diagram of a vehicle-pedestrian impact showing coordinates and variables; *b* is the height of the hood/bonnet leading.

Notation and Impulse-Momentum Equations

b	height of hood/bonnet leading edge (BLE)
d	distance between pedestrian and car at rest
e	coefficient of restitution, pedestrian-vehicle impact
f_c	vehicle-roadway frictional drag coefficient
f_p	pedestrian-roadway frictional drag coefficient
h	height of pedestrian cg at launch
m_c, m_p	mass of vehicle/car and pedestrian, respectively
n, t	normal-tangential coordinates (Fig 3)
P_B	external impulse on vehicle due to braking
P_n, P_t	normal & tangential contact impulse components
R	range of pedestrian trajectory
s	pedestrian travel distance on roadway
s_p	pedestrian throw distance
v_c, v_{c0}	initial speed of vehicle
V_p, v_{p0}	speed of pedestrian at launch
x, y	vehicle heading coordinates Fig (1 & 3)
γ	angle of hood/bonnet (Fig 3)
θ	angle of launch of pedestrian cg
$\mu = f_{pc}$	impulse ratio (effective vehicle-pedestrian

Hood/Bonnet Impact Analysis: Figure 3 shows the coordinates, variables and geometry for the vehicle-pedestrian hood/bonnet impact analysis. The equations that follow are the impulse-momentum solution equations [18] for the final velocity components (upper-case V) of the pedestrian, V_{pn} and V_{pt} and car (vehicle) V_{cn} and V_{ct} in the normal and tangential coordinate system (established by the angle γ of the vehicle's hood/bonnet):

$$V_{pn} = \frac{\bar{m}}{m_p}[(1+e)v_c + P_B/(m_p+m_c)]\cos\gamma \quad (1)$$

$$V_{pt} = \mu[\frac{\bar{m}}{m_p}(1+e)v_c + P_B/(m_p+m_c)]\cos\gamma \quad (2)$$

$$V_{cn} = \{v_c[1-\frac{\bar{m}}{m_c}(1+e)] + P_B/(m_p+m_c)\}\cos\gamma \quad (3)$$

$$V_{ct} = v_c\sin\gamma + P_B\frac{\sin\gamma-\mu\cos\gamma}{m_c} + \mu P_B\frac{\cos\gamma}{m_p+m_c} - \mu\frac{\bar{m}}{m_c}(1+e)v_c\cos\gamma \quad (4)$$

The kinetic energy loss of the vehicle-pedestrian collision is:

$$KE_{loss} = \frac{1}{2}\bar{m}v_{cn}^2(1+e)[(1-e)+2\mu r-(1+e)\mu^2] \quad (5)$$

Equation 5 represents the energy lost in the collision between the vehicle and pedestrian and does not include system kinetic energy lost by braking of the vehicle (if any) during the collision. The variable v_c is the initial speed (lower-case v) of the car and v_{cn} is the closing velocity of the impact, $v_{cn} = v_c \cos\gamma$ (the rate/speed at which the vehicle and pedestrian initially approach each other in the normal direction). Note that if $\gamma = 0$, the crash is referred to as a frontal projection [15]. The preimpact velocity of the pedestrian is assumed to be zero and does not appear explicitly in the equations. The variable e is the coefficient of restitution, $\mu = P_t/P_n$ is the impulse ratio of the collision (effective friction coefficient [18]) and γ is the slope of the hood/bonnet (relative to the vertical y axis). The variables m_p and m_c are the pedestrian and car masses, respectively, $r = v_{ct}/v_{cn}$ and

$$\bar{m} = m_c m_p/(m_c+m_p) \quad (6)$$

The quantity P_B is the impulse due to the tire-road braking force of the vehicle over the duration between initial contact and launch; this is:

$$P_B = -f_c m_c g t_0 \quad (7)$$

where f_C is the tire-road drag coefficient of the vehicle (if any) and t_0 is the duration of forward motion of the vehicle between initial contact to launch. The vertical impulse on the vehicle corresponding to the horizontal impulse, P_B, is considered to be negligible. Dividing Eq 5 by the initial kinetic energy of the vehicle provides the energy loss of the collision expressed as a fraction of the initial kinetic energy of the vehicle. If the impact parameters e and μ are constant for a range of initial vehicle speeds, the percentage energy loss remains constant over that speed range.

Comparison of Pedestrian Throw Model with Multibody Results

Hamacher, et al. [16] present comprehensive results of MADYMO simulations. Results include maximum center-of-gravity height after launch, throw distance, launch speed and launch angle of the pedestrian. These results are obtained from frontal impacts for six types of vehicles, four pedestrian models, four vehicle speeds (20, 30, 35, 40 km/h) averaged over five centralized frontal walking-pedestrian impact positions. The pedestrian models include 6 year-old child, 5%ile female, 50%ile male and 95%ile male. Vehicle physical parameters are provided such as height of the hood/bonnet leading edge and hood/bonnet angle. (Vehicle weights and vehicle front profiles were supplied by the authors.) Pedestrian model physical characteristics are provided including weight, standing cg height and overall height. The forward velocity of the vehicle at the time of pedestrian launch was not given for the MADYMO simulations.

The following presents results of the process of matching MADYMO output with calculations of the Han-Brach Type II model including a vehicle-pedestrian impact model containing the above equations. Specifically, three quantities are found using the following procedure.

- First, an “average vehicle” is defined by averaging the three vehicle physical parameters, weight, hood/bonnet leading edge height and the hood/bonnet angle for all of the six MADYMO simulated vehicles. This gives: m_C = 1642 kg, b = 0.804 m, γ = 71.3°. This is done to allow examination of trends and avoid making comparisons of all individual combinations of vehicles, pedestrians, speeds, etc. [16].
- Next, for each vehicle speed, 20, 30, 35 and 40 km/h, the values of the MADYMO pedestrian launch speed, launch angle and throw distance values are found from the published MADYMO simulations for each pedestrian model.
- Finally, impact parameters, e and $\mu = f_{pc}$ and the pedestrian-ground frictional drag coefficient, f_p (over the distance s in Fig 1), from the enhanced Han-Brach throw model are found using the method of minimum least squares that provides a match of the launch speed, launch angle and throw distance from MADYMO to the launch speed, launch angle and throw distance from the impact throw model.

A constraint on e is imposed during the minimum least-squares process that $0 \le e \le 1$.

Before presenting results, a sample match is carried out for a single, specific MADYMO SUV simulation (not for the average vehicle) as an example to illustrate the matching process. Consider the 50%ile male (mass 75.7 kg, cg height 0.8438 m) hit by a SUV (mass 1700 kg, bonnet leading edge height 0.96 m, hood/bonnet angle 76.6°) traveling at 40 km/h (11.1 m/s). The sum of squares of differences between MADYMO and the throw-distance impact model launch speed, launch angle and throw distance is minimized to find the values of e, f_{pc} and f_p. Results are given in Table 1. Both models give practically identical results for the coefficient of restitution e = 1.00, the vehicle-pedestrian effective friction coefficient f_{pc} = 1.67 and the pedestrian ground friction coefficient f_p = 0.49. The throw-distance impact model gives additional results such as a pedestrian trajectory range of R = 7.2 m, a pedestrian slide distance-to-rest of s = 4.2 m and a difference in rest position distances of the vehicle and the pedestrian of -4.98 m. Appendix A gives the full set of results for this example.

Table 1. Single Case Comparison Results
50%ile male, SUV, 40 km/h (11.1 m/s)

	Launch Speed, m/s	Launch Angle,°	Throw Distance, m
MADYMO:	9.4	17.5	12.4
Impact Model:	9.3	17.5	12.4

[$\mathbf{e = 1.00}$ $\mathbf{f_{pc} = 1.67}$ $\mathbf{f_p = 0.49}$]

Average Vehicle, 50th Percentile and 95th Percentile Males

The matching process between MADYMO results and impact mechanics is carried out for all speeds of the MADYMO 50%ile and 95%ile male runs being hit by a vehicle using the average characteristics of the 6 vehicles. Figure 4 shows the energy lost during the impact between the vehicle and pedestrian. (All matches were “exact” in the sense that the sum of squares of differences was exactly zero between MADYMO results and the Type II impact model.) The impact energy loss increases with vehicle speed. Figure 5 presents the impact coefficients e and f_{pc} corresponding to the MADYMO simulations (and which satisfy the impulse-momentum equations of mechanics).

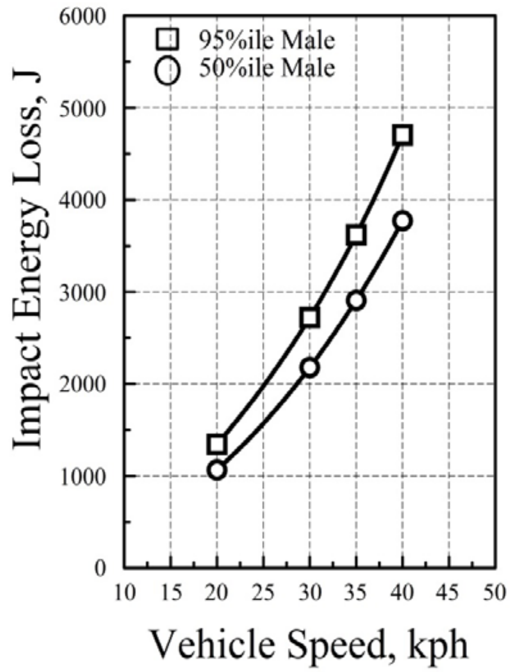

Figure 4. Impact energy loss corresponding to the 50%ile and 95%ile male MADYMO simulations for a vehicle with average characteristics.

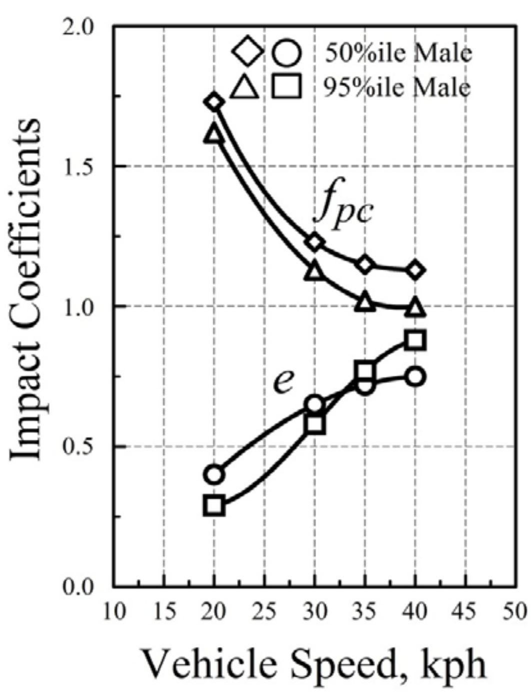

Figure 5. Impact coefficients, *e* and f_{pc}, corresponding to 50%ile and 95%ile male MADYMO simulations for a vehicle with average characteristics.

The values of these coefficients do not remain constant and vary significantly as a function of vehicle speed. The variations are generally smooth and monotonic with the collisions becoming more elastic as speed increases and with the effective friction decreasing between the hood/bonnet and pedestrian. These trends are counterintuitive because at higher speeds mechanical collisions almost always involve increased inelastic effects (greater permanent vehicle deformation and more energy absorbed by the pedestrian — higher injury levels), leading to greater collision energy loss. In almost all mechanical impact processes, the coefficient of restitution decreases with speed [18, 22]. For these reasons, the percent system kinetic energy loss is examined. Specifically, this is the kinetic energy lost in the process of the point mass collision between the vehicle and pedestrian up to the time of launch, Eq 5. (Note that the predicted energy loss values from a point mass impact analysis are higher than from a rigid body impact analysis [17, 18] because the kinetic energy remaining in the bodies in the form of rotational energy is neglected using point-mass theory). The values for the 50%ile and 95%ile male collisions are shown in Figure 6. Although energy loss is higher for the heavier pedestrian, the downward trend with speed is consistent for both data sets. The energy-loss values depend upon the nature of the MADYMO modeling of the elastic-plastic deformation (injury) properties of the pedestrian, the elastic-plastic deformation properties of the vehicle and the interaction contact mechanics between the pedestrian and vehicle.

To determine if the downward trend in energy loss is or is not due to the vehicle-averaging technique the matching process is carried out for the impacts between the 50%ile and 95%ile males and a specific vehicle, namely the Compact Car. The results are given in Figure 7 where the percentage kinetic energy loss has a similar downward trend with speed as in Figure 6.

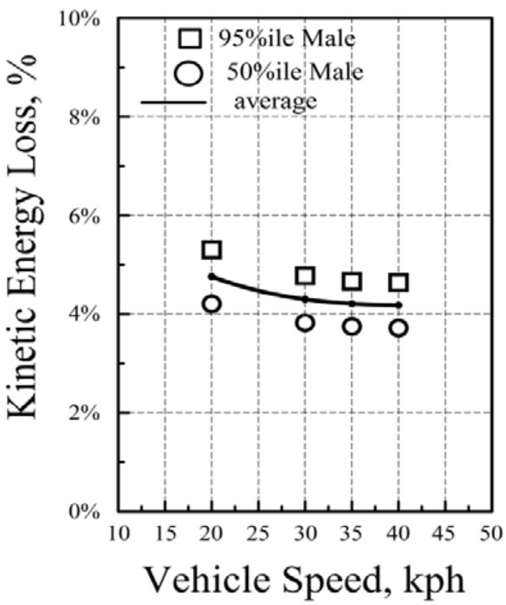

Figure 6. Percentage kinetic energy loss of the impact process between the vehicle and pedestrian up to the time of launch for the average vehicle.

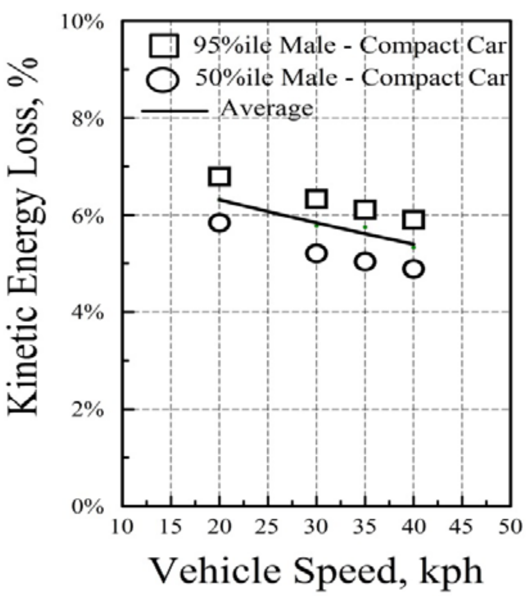

Figure 7. Percentage kinetic energy loss of the impact process between the vehicle and pedestrian up to the time of launch for the MADYMO Compact Car simulations.

Each collision has a critical impulse ratio (tangential impulse divided by the normal impulse for the condition that relative sliding ceases at or before separation) [17, 18, 22]. When relative sliding continues without cessation or reversal through separation, the impulse ratio is equal to the effective coefficient of friction. In all cases, fitting of the MADYMO simulations resulted in an impulse ratio lower than or equal to the critical value.

Pedestrian-ground effective frictional Drag Coefficient: The value of the effective pedestrian-ground friction coefficient between the initial point of ground impact to rest found from the matching process produced an overall average value of f_p = 0.42. This reflects the level of the frictional drag coefficient between the pedestrian and the ground surface used in the MADYMO simulation calculations to determine the total throw distance. A direct comparison between this value and the value used in the simulations cannot be made since this value was not reported in [16].

Analysis of the Trend of Restitution Using Experimental Throw Data

The fitting of data from a Type III model to a Type II model, as presented above, provides a means of evaluation of the Type III model results using the trends of the impact coefficients e and μ. It has been shown that the trend in the restitution from the MADYMO analyses as a function of speed is opposite to the trend generally seen for mechanical impact processes. The trend of the restitution coefficient for pedestrian forward projection impacts specifically is examined here using experimental data.

Toor & Araszewski [23] published a Type I formula for the throw distance of forward projection collisions [15] based on a statistical analysis of numerous experimental tests. The empirical formula is:

$$v_c = 2.29 s_p^{0.6147} \quad (8)$$

where v_c is the speed of the vehicle in m/s and s_p is the throw distance in meters.

Question: For a range of speeds, what coefficients of restitution, e, are necessary for the collision of a

OneBox vehicle and a 6 year-old child to attain the empirical throw distances given by Equation 8?

To answer this question, the value of *e* is found from the enhanced Han-Brach model for the MADYMO OneBox-child vehicle-pedestrian collision conditions to conform to Eq 8 for each speed in the range of 20 to 50 km/h. This process "ties" the conditions of one MADYMO vehicle-pedestrian combination to an experimental base. By carrying out this process using the method of least squares, the change of the coefficient of restitution with speed can be determined. The OneBox vehicle had a mass of 2350 kg. The characteristics of the 6 year-old child included a center-of-gravity height of 0.666 m and a mass of 23.0 kg. A value of f_p = 0.6 (pedestrian-ground friction) was used for all solutions. The OneBox front/grille surface is rounded with no distinct hood/bonnet leading edge and a single slope may not be appropriate for the impact solutions. (MADYMO simulations for this vehicle-pedestrian combination produced launch angles ranging between 9.7° and 10.4°.) For these runs, the launch surface (see Figure 3) was extended down to the grille and given two values, 0° and 10°, to bracket the vehicle's frontal slope at the contact area. The impulse ratio, μ, was approximately zero for all results, that is f_{pc} ~ 0. This means the impact energy loss is due primarily to vehicle-pedestrian direct (normal) contact restitution. Results are shown in Figure 8 where all least-square differences between experimental throw distances and those from the Type II model were identically zero. Complete output of a 50 km/h case is in Appendix B.

For the OneBox-child vehicle-pedestrian collisions to match the experimental forward projection formula (Eq 8, for throw distance) over the speed range from 20 to 50 km/h, the coefficient of restitution decreased from 0.220 to 0.069 for a 0° grille slope and from 0.175 to 0.008 for a 10° grille slope. The percentage kinetic energy loss ranges from 0.92% to 0.96% for 0° front grille slope and 0.91% to 0.94% for the 10° grille slope. In both cases, the kinetic energy loss appears to level off. The trend of the decreasing coefficient of restitution (increasing inelastic effects) and increase of percentage kinetic energy loss with speed matches expectations (based on mechanical impact data) and differs from the results seen from the MADYMO simulations. Because these collisions belong to the forward projection crash category (contact between the pedestrian and the front, grille area of the vehicle) the coefficient of restitution represents the inelastic interaction between the front of the vehicle and the pedestrian.

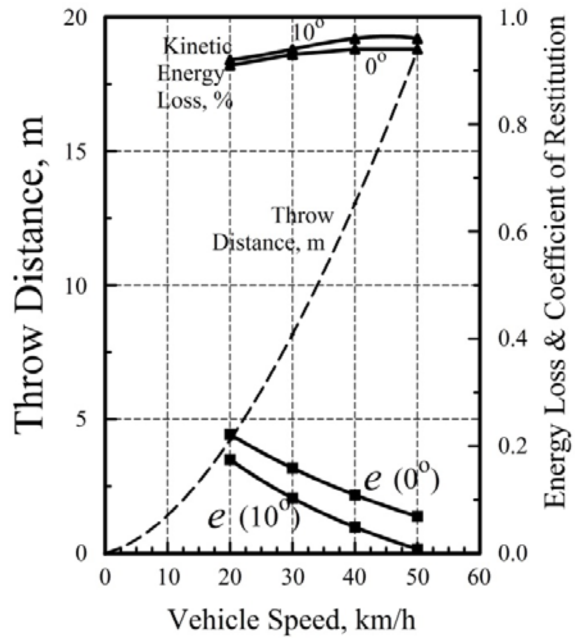

Figure 8. Throw distance, kinetic energy loss and coefficient of restitution for a OneBox-child collision with experimental throw distance for 0° and 10° front grille slope.

Discussion and Conclusions

The main objective of this work was to match (using the minimum least-square method) the enhanced Han-Brach throw model output to a set of MADYMO simulations to determine corresponding impact coefficients and impact energy loss values. It was found that the Type II Han-Brach throw-distance model is capable of accurately matching the MADYMO simulation results such as pedestrian launch speed, launch angle, throw distance, etc.

For a vehicle with averaged characteristics, using the enhanced Han-Brach impact model to determine the impact coefficients (*e* and *μ*) for 50%ile and 95%ile males revealed that the trend of the MADYMO simulations [16] displays increasing elasticity and decreasing effective vehicle-pedestrian contact friction as the vehicle speed increases. Correspondingly, the percentage energy loss of the collision decreases as the vehicle speed increases. Such trends in the coefficients and the energy loss are contrary to what is found from usual mechanical impact processes. It is not clear if such trends are typical of most or all of multibody analyses of vehicle-pedestrian crash simulations.

When the throw distances for the OneBox vehicle and 6 year-old child conditions were made to follow the Toor-Araszewski experimental throw-distance formula, the coefficient of restitution and percentage energy loss trends behaved as expected – decreasing coefficient of restitution with increasing speed and increasing percentage kinetic energy loss.

Although some experimental throw-distance data (Toor-Araszewski formula) were used in Type I to Type II model comparisons to examine the trends in the impact coefficients and the percent energy loss for vehicle-pedestrian collisions, additional experimental validation is necessary to confirm the above results. Based on the results of the work presented here, experimental data should include information necessary to evaluate energy loss of the vehicle-pedestrian contact/interaction process, particularly for wrap collisions.

References

1. Bhalla, K., P. Montazemi, J. Crandall, J. Yang, X. Liu, Y. Dokko, Y. Takahashi, Y. Kikuchi, D. Longhitano, "Vehicle Impact Velocity Prediction from Pedestrian Throw Distance: Trade-Offs between Throw Formulae, Crash Simulators and Detailed Multi-Body Modeling", IRCOBI 30: 14p, 2002.
2. Depriester, J-P, C. Perrin, T. Serre, S. Chalandon, "Comparison of Several Methods for Real Pedestrian Accident Reconstruction, Proc. Int. Tech. Conf. Enhanced Safety Vehicles 2005; 14p.
3. Simms, C. And D. Wood, *Pedestrian and Cyclic Impact*, Springer, 2009.
4. Wood, D. P., C. K. Simms, and D. G. Walsh, "Vehicle–pedestrian collisions: validated models for pedestrian impact and projection", DOI: 10.1243/095440705X6703, Proc. IMechE. **219** Part D: *J. Automobile Engineering* D11504, 2005.
5. Russell, C. Gregory, Pedestrian Formulas for Excel, Lawyers & Judges Publishing Company.
6. Wood, D. and C. Simms, "A Hybrid Model for Pedestrian Impact and Projection," I J Crashworthiness, Vol. 5, No. 4, pp 393-403, UK, 2000.
7. Wood, D. and D. Walsh, "Pedestrian forward projection impact," I J Crashworthiness, Vol. 7, No. 3, 2002.
8. Han, I and R. M. Brach, "Throw Model for Frontal Pedestrian Collisions", Paper 2001-01-0898, SAE 2001 Congress, Detroit, MI., March, 2001.
9. Han, I. and R. M. Brach, "Impact Throw Model for Vehicle-Pedestrian Collision Reconstruction," Journal of Automobile Engineering (Proceedings of the Institution of Mechanical Engineers Part D), Vol 216, No 6, June 2002, pp 443-453.
10. PC-Crash, www.pc-crash.com.
11. MADYMO, www.tassinternational.com.
12. D. Vangi, "A fuzzy approach to reconstructing vehicle–pedestrian collisions", *Vehicle System Dynamics: International Journal of Vehicle Mechanics and Mobility*, 47:9, 1115-1135, DOI: 10.1080/00423110802460689, 2009.
13. Han, I. "Fuzzy Estimation of Vehicle Speed in Pedestrian Collision Accidents", *International Journal of Automotive Technology*, Vol. 14, No. 3, pp. 385-393, DOI 10.1007/s12239-013-0042-y (2013).
14. Eubanks, J., P. Hill,, D. Casteel, S. Solomon, R. Malmsbury, G. Schmunk, Pedestrian Accident Reconstruction and Litigation, 2nd Ed, Lawyers & Judges Publishing Company, 2002.
15. Ravani, B., D. Brougham, R. Mason, "Pedestrian post-impact kinematics and injury patterns", Paper 811024, SAE International, 1981.
16. Hamacher, M., L. Eckstein and R. Paas, "Vehicle Related Influence of Post-Car Impact Pedestrian Kinematics on Secondary Impact", IRC-12-78, IRCOBI Conference 2012.
17. Brach, Raymond and Matthew Brach, *Vehicle Accident Analysis and Reconstruction Methods*, 2nd Ed, SAE International, April, 2011.
18. Brach, R. M., *Mechanical Impact Dynamics*, Revised Ed, Brach Engineering, 2007.

19. van Rooij, L, K Bhalla, M Meissner, J Ivarsson, J Crandall, Pedestrian Crash Reconstruction Using Multi-body Modeling with Geometrically Detailed, Validated Vehicle Models and Advanced Pedestrian Injury Criteria, Paper Number 468.
20. Yang JK, and P. Loevsund, Development and validation of a human-body mathematical model for simulation of car-pedestrian collisions, Proc. IRCOBI 1997; 25: 133-149.
21. Elliot, J., M Lyons, J Kerrigan, DP Wood, C. Simms, Predictive capabilities of the MADYMO multibody pedestrian model: Three-dimensional head translation and rotation, head impact time and head impact velocity, Proceedings of the Institution of Mechanical Engineers, Part K, Journal of Multi-body Dynamics September 2012 vol. 226 no. 3 266-277.
22. Brogliato, B. *Nonsmooth Mechanics*, Models Dynamics and Control, 2nd Ed., Springer, 1999.
23. Toor, A. & M. Araszewski, “Theoretical vs. Empirical Solutions for Vehicle/Pedestrian Collisions”, Paper 2003-01-0883, SAE International, 2003.

Contact

Raymond M. Brach, PhD
P.O. Box 839
Notre Dame, IN 46556-0839
rbrach@nd.edu

X. Appendix A. Full Results of Single-Case, 50%ile Male, SUV, Pedestrian Impact Throw Model

	A	B	C	D	E	F
1	50%ile M fit SUV 40.xls			**Analysis of Pedestrian Throw Distance from Initial Conditions**		
2	10/21/2015					
3	NOTATION, COORDINATES, UNITS & VARIABLES:				**UNIT CONVERSION**	
4	x	-		coordinate parallel to ground		
5	y	-		coordinate perpendicular to ground		
6					SI	
7	**INPUT INFORMATION (KNOWNS):**					
8	a_2	0.80		f_c, deceleration of vehicle over distance s_2, g's		
9	f_p	0.49		drag resistance coefficient of pedestrian over distance s		
10	g	9.81	m/s²	acceleration of gravity		
11	CG	0.959	m	standing height of pedestrian center of gravity	h	0.96
12	s_1	0.00	m	distance of travel of vehicle at uniform speed (no braking)	x_L	1.11
13	v_{c0}	11.11	m/s	initial speed of vehicle	γ	76.60
14		40.0	kph	initial speed of vehicle		
15	BLE	0.966	m	Bonnet Leading Edge height, b		
16	e	1.00		coefficient of restitution, vehicle-pedestrian hood/bonnet		
17	HBSL	76.60	deg	Hood/Bonnet slope from vertical		
18	φ	0.00	deg	road grade angle		
19	f_{pc}	1.67		friction coeff - ped to launch surface		
20	m_c	1700.0	kg	mass of vehicle, weight / g		
21	m_p	76.70	kg	mass of pedestrian, weight / g		
22						
23	**OUTPUT INFORMATION (UNKNOWNS):**					
24	v'_{c0}	9.96	m/s	velocity of vehicle after impact with pedestrian		
25	v_{p0}	9.27	m/s	initial speed of pedestrian		
26	θ	17.47	deg	launch angle of pedestrian		
27	R	7.16	m	range of pedestrian throw, launch to ground impact		
28	t_{p1}	0.91	s	time from impact to pedestrian initial contact with ground		
29	s	4.13	m	pedestrian ground contact distance, impact to rest		
30	s_p	12.40	m	throw distance; total distance from initial contact to pedestrian rest		
31	t_p	2.22	s	total time of travel of pedestrian, initial contact to rest		
32	t_{c1}	0.11	s	time of travel of vehicle to travel from initial contact to $s_0 + s_1$		
33	s_0	1.11	m	distance of travel of vehicle with pedestrian contact		
34	s_2	6.31	m	distance of travel of vehicle with uniform deceleration, a_2		
35	s_{veh}	7.42	m	total distance of travel of vehicle, $s_{veh} = s_0 + s_1 + s_2$		
36	P_B	-1333.70	N-s	Impulse due to Brake Application		
37	t_c	1.38	s	vehicle travel time, initial contact to rest		
38	d	-4.98	m	distance between rest positions of vehicle and pedestrian		

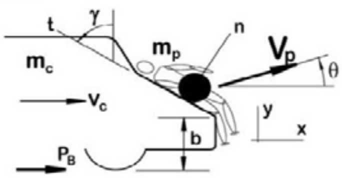

XI. Appendix B. Results of Single-Case, 6 year-old Child, OneBox Vehicle, Pedestrian Impact Throw Model

	A	B	C	D	E	F
1	6 Y-O child 1box Toor.xls			**Analysis of Pedestrian Throw Distance from Initial Conditions**		
2	10/21/2015					
3	NOTATION, COORDINATES, UNITS & VARIABLES:				**UNIT CONVERSION**	
4	x	-		coordinate parallel to ground		
5	y	-		coordinate perpendicular to ground		
6					SI	
7	**INPUT INFORMATION (KNOWNS):**					
8	a_2	0.70		f_c, deceleration of vehicle over distance s_2, g's		
9	f_p	0.60		drag resistance coefficient of pedestrian over distance s		
10	g	9.81	m/s²	acceleration of gravity		
11	CG	0.666	m	standing height of pedestrian center of gravity	h	0.67
12	s_1	0.00	m	distance of travel of vehicle at uniform speed (no braking)	x_L	0.00
13	v_{c0}	13.89	m/s	initial speed of vehicle	γ	0.00
14		50.0	kph	initial speed of vehicle		
15	BLE	1.021	m	Bonnet Leading Edge height, b		
16	e	0.069		coefficient of restitution, vehicle-pedestrian hood/bonnet		
17	HBSL	58.80	deg	Hood/Bonnet slope from vertical		
18	φ	0.00	deg	road grade angle		
19	f_{pc}	0.00		friction coeff - ped to launch surface		
20	m_c	2360.0	kg	mass of vehicle, weight / g		
21	m_p	23.00	kg	mass of pedestrian, weight / g		
22						
23	**OUTPUT INFORMATION (UNKNOWNS):**					
24	v'_{c0}	13.74	m/s	velocity of vehicle after impact with pedestrian		
25	v_{p0}	14.70	m/s	initial speed of pedestrian		
26	θ	0.00	deg	launch angle of pedestrian		
27	R	5.42	m	range of pedestrian throw, launch to ground impact		
28	t_{p1}	0.37	s	time from impact to pedestrian initial contact with ground		
29	s	13.35	m	pedestrian ground contact distance, impact to rest		
30	s_p	18.76	m	throw distance; total distance from initial contact to pedestrian rest		
31	t_p	2.60	s	total time of travel of pedestrian, initial contact to rest		
32	t_{c1}	0.00	s	time of travel of vehicle to travel from initial contact to $s_0 + s_1$		
33	s_0	0.00	m	distance of travel of vehicle with pedestrian contact		
34	s_2	13.76	m	distance of travel of vehicle with uniform deceleration, a_2		
35	s_{veh}	13.76	m	total distance of travel of vehicle, $s_{veh} = s_0 + s_1 + s_2$		
36	P_B	0.00	N-s	Impulse due to Brake Application		
37	t_c	2.00	s	vehicle travel time, initial contact to rest		
38	d	-6.00	m	distance between rest positions of vehicle and pedestrian